Electroactivity of superoxide anion in aqueous phosphate buffers analyzed with platinized microelectrodes

Pauline Lefrancois, Fanny Girard-Sahun, Vasilica Badets, Franck Clement, Stéphane Arbault

Full Paper

Wiley Online Library

ELECTROANALYSIS

DOI: 10.1002/elan.202060456

Electroactivity of Superoxide Anion in Aqueous Phosphate Buffers Analyzed with Platinized Microelectrodes

Pauline Lefrançois[+],[a, c] Fanny Girard-Sahun[+],[a, b, c] Vasilica Badets,[a, c] Franck Clément,[b] and Stéphane Arbault*[a]

Abstract: The reactivity of platinized ultramicroelectrodes (Pt-black UMEs) towards superoxide anion $O_2^{\bullet-}$, an unstable Reactive Oxygen Species (ROS), and its relatives, H_2O_2 and O_2, was studied. Voltammetric studies in PBS demonstrate that Pt-black UMEs provide: i) a well-resolved reversible redox signature for $O_2^{\bullet-}$ detected in both alkaline and physiological buffers (pH 12 and 7.4); ii) irreversible oxidation and reduction waves for H_2O_2 at pH 7.4. The oxygen reduction reaction (ORR) at Pt-black surfaces solely yields H_2O_2 (2 electrons/2 H^+) at physiological pH. Consequently, Pt-black UMEs allow to sense different ROS including superoxide anion for future biomedical or physico-chemical investigations.

Keywords: superoxide · ultramicroelectrode · hydrogen peroxide · reactive oxygen species · cold atmospheric plasma

1 Introduction

The Reactive Oxygen and Nitrogen Species (ROS, RNS, merged as RONS) are known to play crucial roles in multiple biological processes, including innate immunity, redox signaling, vasodilation, neuro-modulation, carcinogenesis, etc. [1–5]. ROS are produced by aerobic cells owing to diverse enzymatic systems (NADPH oxidase, Xanthine oxidase, etc.) and by side reactions such as during the reduction the conversion of dioxygen (O_2) to water by the mitochondrial respiratory chain (semi-quinone intermediate reduction). Bioactive ROS mostly comprise superoxide anion ($O_2^{\bullet-}$), hydrogen peroxide (H_2O_2), hydroxyl radical ($HO^{\bullet}$) and singlet oxygen ($^1O_2$) both produced under the presence of catalysts. The radicals are by nature very reactive and unstable in physiological conditions: the lifetime of $HO^{\bullet}$ is about 1 ns [6]; $O_2^{\bullet-}$ disproportionation occurs at rate constants of $5.10^{-5}\,M^{-1}{\cdot}s^{-1}$ and $10^{-9}\,M^{-1}{\cdot}s^{-1}$ at pH 7.4, either spontaneously or when catalyzed by superoxide dismutases (SOD), respectively. The disproportionation follows the reaction [7]:

$$2O_2^{\bullet-} + 2H^+ \rightarrow O_2 + H_2O_2 \quad (1)$$

H_2O_2 is stable over hours in aqueous solution at pH 7.4 and is degraded in presence of metal ion traces (iron or copper ions) [8,9], and catabolic enzymes, namely catalase and peroxidases. The ROS can be involved further in reactions with nitrogen derivatives including nitric oxide ($NO^{\bullet}$) to form highly reactive, nitrosative and nitrative species, such as the peroxynitrite anion ($ONOO^-$), nitrogen dioxide (NO_2) and the nitrosonium cation (NO^+) [10,11].

The RONS can also be produced by other physico-chemical processes involved in atmospheric pollution or developed for sterilization, chemical reactions, etc. [12–15] This is the case of Cold Atmospheric Plasmas (CAPs), which are complex ionized gases composed of electrons, neutral atoms or molecules, ions and excited atoms or molecules. CAPs can be produced experimentally at atmospheric pressure and room temperature and are used for a large range of biomedical applications: skin regeneration, skin tumor treatment, teeth whitening, etc. [15–17]. The majority of the observed biological effects induced by CAPs are due to RONS.

For these reasons, there is still a large interest for the detection and quantification of the biologically active RONS. However, this remains a challenge, mainly because their short lifetime does not allow enough accumulation. Therefore, their subsequent detection by analytical techniques is very limited [18]. This is partic-

[a] P. Lefrançois,[+] F. Girard-Sahun,[+] V. Badets, S. Arbault
Univ. Bordeaux, Bordeaux INP
CNRS UMR 5255, ISM, groupe NSysA
33400 Talence, France
E-mail: stephane.arbault@u-bordeaux.fr
[b] F. Girard-Sahun,[+] F. Clément
UPPA, IPREM
CNRS UMR 5254
2 avenue Président Angot
64000 Pau, France
[c] P. Lefrançois,[+] F. Girard-Sahun,[+] V. Badets
Chemistry Department, University of Antwerp
Campus Drie Eiken Universiteitsplein 1, Belgium.
and
Department of Biochemistry, University of Groningen
Groningen Biomolecular Sciences and Biotechnology Institute
Nijenborgh 4, 9747 AG Groningen, The Netherlands
and
University of Strasbourg, Chemistry Institute
UMR CNRS 7177
4 rue Blaise Pascal, CS 90032, 67081 Strasbourg cedex, France
[+] These two authors contributed equally to the paper.

ularly true when RONS are produced in aqueous buffers under CAPs exposure. We have recently reported the electrochemical detection of kinetically stable species, including H_2O_2, NO_2^- and NO_3^- species, accumulating in PBS during its constant exposure to a CAP [19]. The detection in plasma-treated solutions of H_2O_2 at concentrations reaching hundreds of µM [20,21], as well as the detection of peroxynitrite $ONOO^-$ (tens of µM) by UV-visible absorption spectroscopy [19,20] have strongly suggested the prior existence of superoxide in these solutions. Unfortunately, the hypothesis was not confirmed since the direct detection of $O_2^{\bullet-}$ in aerobic and physiological conditions remains very challenging. The objective of the present work is to propose an electroanalytical approach to go beyond this limitation.

A wide variety of electrochemical sensors for the detection of RONS have been reported, particularly based on redox enzymes (peroxidase, catalase, etc.) [22–25]. The specific detection of $O_2^{\bullet-}$ was shown by using cytochrome *c*-modified gold electrodes [26]. Ultramicroelectrodes (UMEs) which carbon or platinum surface could be modified by platinum nanostructured rough deposits, quoted as platinum black (Pt-black coating) were later developed [27,28]. Their electrocatalytic properties provide UMEs with the ability to selectively detect several ROS and RNS [29–31]. In addition, platinized UMEs are particularly useful for sensitive measurements in micrometric volumes including at single cells [32] and in microsystems (channels and chambers) [33–36]. Pt-black UMEs display a fast response-time and offer linear current variations over large concentration domains of e.g. H_2O_2 (from tens of nM to mM) [37]. In addition, we recently observed that Pt-black UMEs allow to detect superoxide anion in alkaline conditions (PBS at pH 12) [37].

The aim of this paper is to further investigate the electroanalysis of $O_2^{\bullet-}$ as function of the pH in phosphate buffers (pH 12 to 7.4). The reactivity of Pt black UMEs towards the by-products of superoxide disproportionation, H_2O_2 and O_2, was studied at pH 7.4 for each species and in solutions containing both species. We demonstrate that superoxide and hydrogen peroxide can be detected selectively at different potentials in aerobic PBS. Finally, we show the direct monitoring of superoxide, when produced and accumulating in alkaline PBS exposed to a CAP. Thus, this study will serve as a reference work to decipher on the complex production of RONS by CAPs and biological sources as well.

2 Experimental

2.1 Chemicals

PBS solution at 10 mM, pH 7.4, was prepared by dissolving the content of a ready-made salt mix (ref. P5368, Sigma Aldrich) in 1 L of pure milliQ water (Millipore, Integral 3, 0.22 µm MilliPak filter). PBS solution at 10 mM and pH 12 was prepared by additions of 1 M sodium hydroxide in PBS pH 7.4 (10 mM). Solutions of H_2O_2 were prepared by dilutions of a 100 mM stock solution in PBS, freshly prepared from a 9.8 M commercial solution (30 % hydrogen peroxide, Sigma). A stock solution of superoxide was prepared by solubilizing potassium dioxide (ref. 278904 Sigma Aldrich) in ice-cold 30 mM NaOH. The obtained concentration was calculated following a protocol reported elsewhere [37,38]. Briefly, a ~1 M superoxide stock solution was prepared, which corresponds to 5 M KO_2 (Caution! Potassium superoxide reacts violently with water). The 1:5 ratio was proposed by Marklund *et al.* and originates from the high reactivity of $O_2^{\bullet-}$ [17]. Superoxide dismutase (ref. S5639, Sigma Aldrich) stock solution was prepared at 30 kU.mL^{-1} in PBS (10 mM, pH 7.4), aliquoted and stored at −20 °C. Aliquots were thawed prior to use.

2.2 Fabrication and Surface Modification of UMEs

UMEs were prepared by heat-sealing Pt micro-wires (25 µm diameter, 99 % purity, Goodfellow) in glass capillaries (1 mm diameter, WPI) (Figure 1). Each UME was polished with coarse- and fine-grade polishing papers before use or further surface modification. Platinum-black electrodeposition (Pt-black) on UME surface was obtained in potentiostatic mode, at a potential of −0.06 V vs. Ag/AgCl/NaCl 3 M, by reducing a hydrogen hexachloroplatinate solution (115 mM in 10 mM PBS, pH 7.4 with 0.76 mM of lead acetate). The electrodeposition was stopped when the total reduction charge reached ~0,1 µC µm^{-2} (37 µC total charge), which corresponds to a previously defined optimum for the detection of hydrogen peroxide by Pt-black UMEs [39] (Figure 1C).

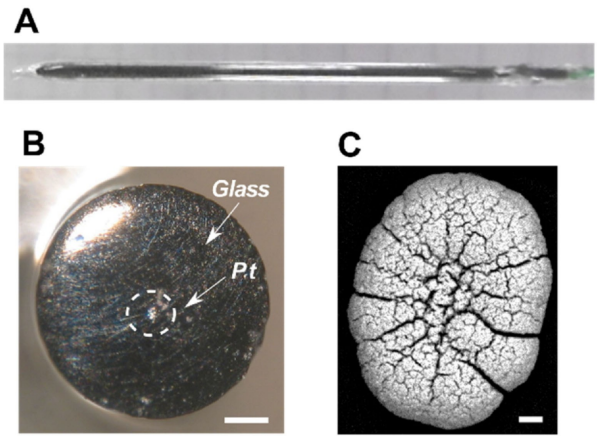

Fig. 1. Multiscale view of a platinized platinum ultramicroelectrode (Pt wire Ø 25 µm, total external diameter 1 mm) used as WE in the experiments. (A) Side view of the whole electrode. (B) Top view of the electrode. The Pt wire (encircled) is sealed in a glass capillary. Scale bar = 100 µm. (C) Platinum-black nanostructure observed by scanning electron microscopy. Scale bar = 5 µm.

2.3 Electrochemical Measurements

2.3.1 Cyclic Voltammetry

All the characterizations of ROS electrochemical responses were achieved by cyclic voltammetry (CV). Experiments were performed using a gas tight electrochemical cell comprising typically 20 mL of solution. The three electrodes (WE: Pt-black UME, REF: Ag/AgCl wire, CE: Pt wire) were inserted in the septum stopper of the electrochemical cell. When needed, a slight gas flow was injected using a needle for 7–10 min to saturate the solution with either nitrogen or oxygen. The effective solution saturation in N_2 or O_2 was estimated by following the signal evolution in CV. When no modification of the solubilized gas was performed, we will quote the experimental condition as 'aerated' or will not specify it. Measurements were obtained in steady-state conditions at a 20 $mV\,s^{-1}$ scan rate, within different potential ranges, specified for each experiment. All the potentials are computed with respect to an Ag/AgCl (saturated KCl solution)-type reference electrode. All electrochemical measurements were carried out using a bipotentiostat (BioLogic, VSP-300, EC-Lab software) equipped with low current modules and filters set at 5 Hz. The analyses were performed in a Faraday cage to minimize the electric noise.

2.3.2 Collector-generator Experiment

For collector-generator experiments, we prepared platinized carbon fiber-based UMEs, which outer diameter was smaller and easier to manipulate. To prepare a carbon UME, an individual carbon fiber (10 µm diameter, Cytec Engineered Materials, ref. Thornel P-55S) was inserted in a glass capillary (1 mm diameter, WPI) and sealed by heat pulling (Narishige, model PC10). The protruding part of carbon fiber was insulated by electrochemical deposition of poly-oxyphenylene (see [40] for details). The tip of the insulated carbon fiber was then polished at a 45° angle on a microgrinder (WPI, model 48000, 1 µm roughness) to expose a clean, elliptical carbon surface. The polished carbon surface was then platinized following the same procedure as for Pt UMEs described in the previous section.

In these experiments, two different electrochemical measurements were performed at each UME, by using cyclic voltammetry on one side (from +0.16 to −0.34 V) and chrono-amperometry at a fixed potential (+0.35 V) on the other one, or chrono-amperometry at a different potential on each UME. A three-electrode electrochemical configuration was used for each UME, composed of the platinized carbon UME as working electrode, an AgCl-coated-Ag wire as pseudo-reference electrode (REF; 1 mm diameter) and a Pt wire as counter electrode (CE; 1 mm diameter). Each UME was coupled to an individual CE whereas a common REF was used for the two UMEs.

An inverted microscope (Leica STP 6000, 20x objective) was used to observe the position of one UME to the other. The experiment was carried out on a clean microscope slide on which a rectangular PDMS frame was placed. All the electrodes were positioned in 1 mL of PBS solution (10 mM, pH 7.4, Sigma). The position of the two UMEs was set with two micromanipulators (ThorLabs, PCS-5200) facing each other at a few micrometers distance.

2.3.3 Analysis in Solution Exposed to a Cold Atmospheric Plasma

The plasma setup used in these experiments has been described previously [20,21]. Briefly, a surrounding gas device allows to control the gaseous environment of the gas phase (plasma). We used helium He as the working gas (1.67 slm rate) and the environment gas was composed of 100 % N_2 (0.03 slm rate; Linde, 99.9995 %), for a total gas flow of 1.7 slm. The production of ionization waves was achieved using a pulsed high voltage power supply with rise and fall times of pulses in the order of 100 ns. The electrical parameters are as following: positive pulses of 7.5 kV amplitude, 1 µs duration, 10 kHz repetition frequency and 1 % duty cycle. 6 mL of PBS at pH 11 was exposed to the plasma in a homemade quartz cuvette (external diameter 44 mm, inner diameter 41 mm, depth 40 mm). A distance of 20 mm was fixed between the end tube of the plasma device and the solution. Moreover, the cuvette was placed over a metallic support connected to the ground in order to ensure a constant potential to the sample. The working WE Pt-black UME, as well as the REF and CE electrodes, were inserted within two insulated-earthed containers in order to protect them from the surrounding high electric field transported by the plasma. Each container was made of a quartz glass capillary (few centimeters long, internal diameter 7–9 mm) covered by a conductive sheath connected to the ground of the building, and covered by an insulating layer of retractable polymer sheath for power cables. Containers (first with WE and REF; second with CE) were placed in the PBS solution and continuous CV was performed at the WE before and during the solution exposure by the CAP to monitor the generation of ROS including superoxide.

3 Results and Discussion

3.1 Redox Behavior of Hydrogen Peroxide and Oxygen in PBS pH 7.4

3.1.1 Redox Behavior of H_2O_2

First, the electrochemical reactivity of Pt-black UMEs was analyzed in H_2O_2 solutions. We previously reported the characterization of the oxidation waves of hydrogen peroxide on these surfaces for large concentrations (up to 100 mM) and positive potential ranges [37]. Herein, we focused on lower concentrations (< 1 mM) in order to get

closer to the range of concentrations measured in PBS exposed to CAPs [20,21]. Cyclic voltammetry analyses were performed between −0.2 V and +0.5 V, allowing to observe both the reduction and oxidation processes for H_2O_2. Results are depicted on Figure 2. We observe in these conditions two well separated, irreversible oxidation and reduction waves, which plateaus start around +0.35 V vs. Ag/AgCl and −0.15 V vs. Ag/AgCl, respectively. We hypothesize that the oxidation reaction of H_2O_2 follows the equation (Equation 2):

$$H_2O_2 \rightarrow O_2 + 2H^+ + 2e^- \quad (2)$$

(redox couple O_2/H_2O_2), while the reduction of H_2O_2 follows (Equation 3):

$$H_2O_2 + 2H^+ + 2e^- \rightarrow 2H_2O \quad (3)$$

(redox couple H_2O_2/H_2O). Indeed, the amplitudes of both waves are directly dependent on the concentration of H_2O_2. The plateau current of each wave was plotted as a function of H_2O_2 concentration (see Figure S1). The response follows a linear evolution both in oxidation and reduction, providing good calibration curves for Pt-black UMEs in each potential domain. However, the slope is slightly lower in reduction, possibly because of two processes: the interference from phosphate anions, which adsorb on platinum and compete with other species; the formation of platinum oxides and their involvement in the oxidation process [41]. Nevertheless, both waves display similar current ranges for the same concentrations, showing that 2 electrons are involved in each electrochemical reaction. This is very unlikely, thermodynamically and kinetically, at physiological pH that 1e-reduction or oxidation processes occur. The proton concentration is sufficiently high to drive the reactions. Kinetically, hydroxyl radicals would not be stable enough to be observed, as well as for superoxide radical anions, which is demonstrated in the ensuing collector-generator experiments. In addition, H_2O_2 is a redox amphoteric species, thus the same diffusion coefficient applies for the reduction and oxidation reactions.

3.1.2 Redox Behavior of O_2

The second set of experiments was designed to study the electroactivity of dioxygen on Pt-black UMEs in the potential range of hydrogen peroxide reactions. CV responses were recorded in PBS solutions containing different amounts of dissolved oxygen: either aerated, N_2- or O_2- saturated. Results are presented on Figure 3.

A reduction wave, which starts at 0 V and is kinetically slow, appears when the PBS solution is saturated with O_2, whereas N_2-saturated PBS response shows solely the PBS background current (capacitive signal). The aerated PBS response shows an intermediate response, corresponding to the 220 µM concentration of solubilized dioxygen in equilibrium in aerated solutions. The Oxygen Reduction Reaction (ORR) catalyzed by platinum-based electrodes is a well-studied reaction with a major focus on the products, being either H_2O_2 or H_2O in aqueous solutions [42–45]. However, little is known about the ORR product on Pt-black surfaces, which have rarely been used for that purpose.

In this study, H_2O_2 and O_2 are key species (mother or daughter species of superoxide anion). Therefore, it was necessary to know what the product of ORR [46,47] in our experimental conditions is (PBS pH 7.4, Black-Pt UMEs). To do so, we designed a collector-generator experiment that aimed to detect *in situ* the product of ORR [48] (Figure 4). In this experiment, a reduction reaction and an oxidation reaction can be performed simultaneously but independently at the surface of two electrodes (Figure 4A). When the two electrodes are close enough, their respective diffusion layers overlap. It allows

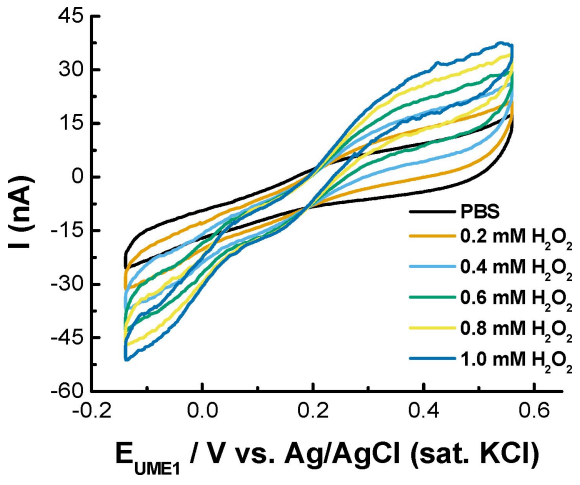

Fig. 2. Cyclic voltammetry responses of H_2O_2 solutions using Pt-black UMEs. H_2O_2 solutions from 0.2 to 1 mM concentration are prepared in aerated physiological PBS at pH 7.4. Scan rate: 20 mV s^{-1}.

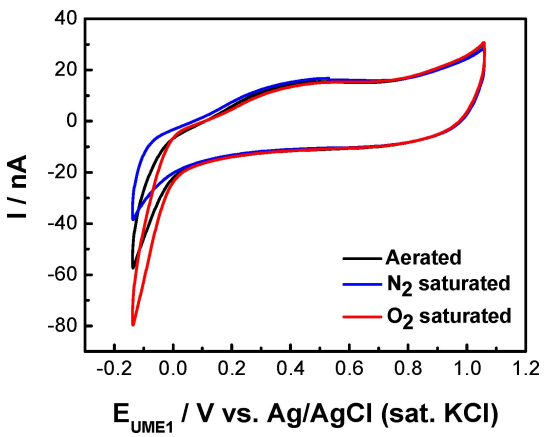

Fig. 3. Cyclic voltammetry responses on a Pt-black UME of aerated (black trace), N_2 (blue trace) and O_2 (red trace) saturated PBS solutions (10 mM, pH 7.4). Scan rate: 50 mV s^{-1}.

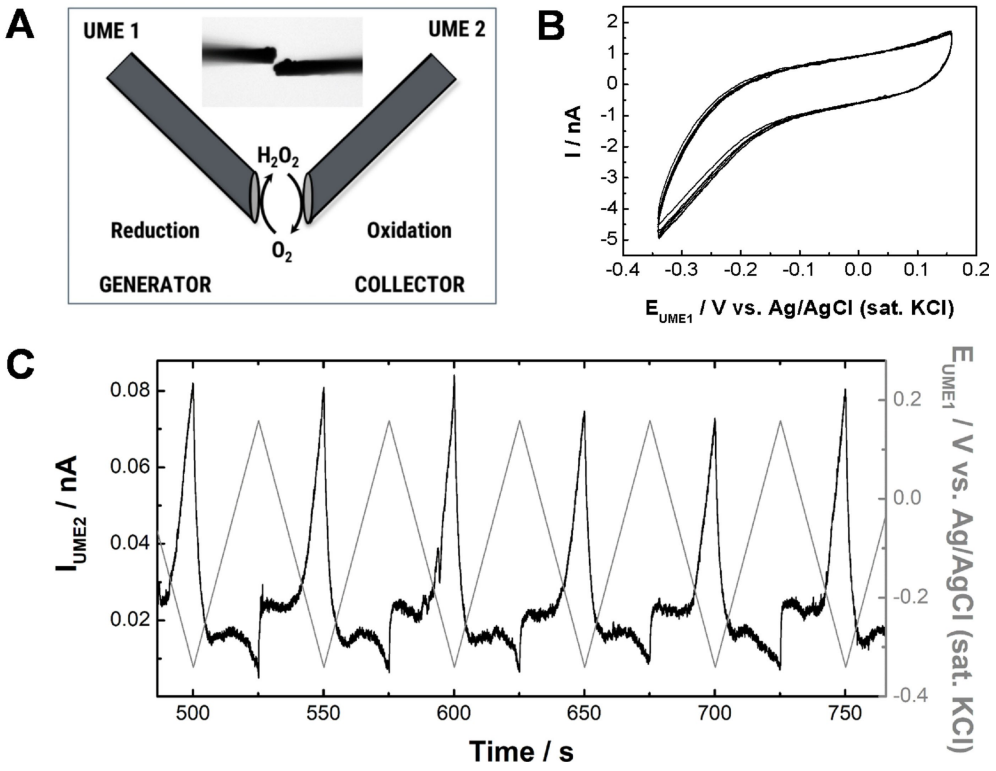

Fig. 4. A collector-generator experiment with two UMEs was performed to decipher on the ORR mechanism at Pt-black surfaces. A. Schematic representation describing the experiment principle. Inset: Image of the two electrodes used for the generator-collector experiment observed in transmitted light (bright field, inverted microscope). The distance between the two UMEs was set using two micromanipulators. B. Cyclic voltammogram of UME 1 at potentials varying between +0.16 V to −0.34 V (generator) at 50 mV s^{-1}. C. The induced current is recorded on UME 2 (black trace). The potential variations applied to the generator are displayed (dashed grey trace) to correlate with the collector signal.

the electro-generation of a species on one electrode (generator) that is detected on the other electrode (collector). Cyclic voltammetry measurements were made at 20 mV s^{-1}, between +0.16 V and −0.34 V vs. Ag/AgCl, in order to reduce O_2 on UME 1 (Figure 4A, left: generator), while current intensity variations were monitored by chrono-amperometry on UME 2 (Figure 4A, right: collector) at the oxidation potential of H_2O_2 (+0.35 V vs. Ag/AgCl). The reduction wave detected on UME 1 is similar to the one observed in Figure 3 (Figure 4B). This process generates a species that is detected on UME 2, as shown by the simultaneous current variations (Figure 4C). The only candidate is H_2O_2 in comparison with our previous studies [28,49,50].

Additionally, we confirmed that the species produced at UME 1 is effectively diffusing in solution before being detected at UME 2 by varying the distance between UME 1 and UME 2 (see Figure S2). In this experiment, both UME were set at a fixed potential: a continuous generation on UME 1 (chronoamperometry at −0.34 V vs. Ag/AgCl) occurred simultaneously with a continuous collection on UME 2 (chronoamperometry at +0.35 V vs. Ag/AgCl). When the distance between the two electrodes was about 1 µm, the current on UME 2 was maximum (~0.03 nA) whereas it decreased drastically when the distance was superior to 10 µm (~0.015 nA, i.e. close to the background current). Indeed, the diameter of the electrode being of 25 µm, the size of the diffusion layer is about 10–15 µm (in the Nernst approximation). Therefore, the species produced by the reduction of O_2 on UME 1 is no longer detected on UME 2. Overall, the collector-generator experiments demonstrated that H_2O_2 is the major product of the O_2 reduction reaction on Pt-black electrodes at physiological pH (PBS, pH 7.4).

3.1.3 Redox Behavior of H_2O_2 and O_2 Mixture

From results depicted on Figures 2 and 3, we observe that both O_2 and H_2O_2 are reduced on Pt-black electrodes at similar potentials, below 0 V vs. Ag/AgCl. As these two species should be produced together during superoxide disproportionation (Equation 1), we studied how they could possibly be discriminated. To answer this question, cyclic voltammetry experiments were realized in N_2- and O_2-saturated H_2O_2 solutions (1 mM) between −0.2 V and +0.5 V (Figure 5).

When the H_2O_2 solution was saturated with dioxygen, the reduction current increased compared to the N_2-saturated one. It is clear from these curves that the reduction wave of oxygen superimposes with the one of

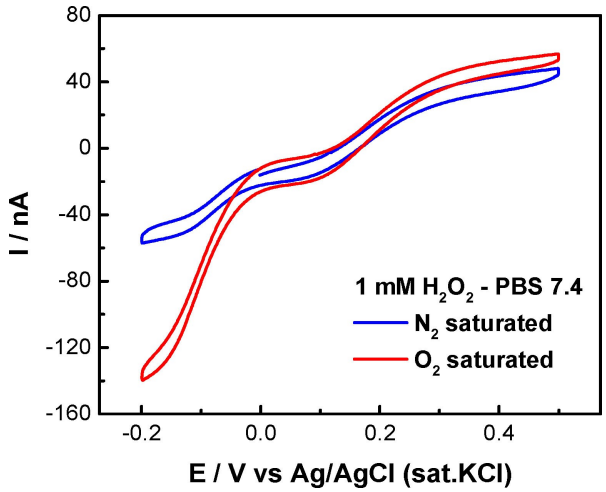

Fig. 5. Cyclic voltammetry responses on Pt-black UMEs of N_2- (blue trace) and O_2- (red trace) saturated H_2O_2 solutions (1 mM) prepared in PBS (10 mM, pH 7.4). Scan rate: 20 mV s^{-1}.

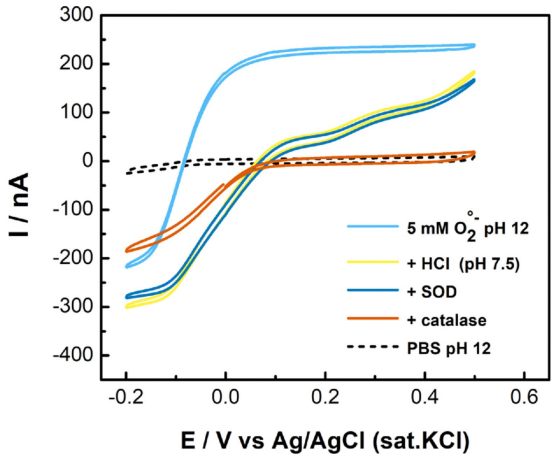

Fig. 6. Evolution of the cyclic voltammetry response (on Pt-black UMEs) in a superoxide basic solution (blue trace, t = 0), when pH is changed to physiological values (yellow trace), followed by SOD (55 U mL^{-1} final, purple trace, t = 13 min) and catalase (> 100 U mL^{-1} final, orange trace, t = 17 min) additions. Scan rate: 20 mV s^{-1}.

hydrogen peroxide, though a slight shift may be distinguished; the plateau potential for O_2 is observed ~30 mV further than the one of H_2O_2. Nevertheless, the total faradaic current at −0.2 V is indeed the sum of at least the two reduction currents of hydrogen peroxide and dioxygen. Consequently, the two species cannot be discriminated based solely on electro-reduction responses although figure 5 shows also that in the potential range of +0.1 V and +0.5 V, the oxidation current is specific to H_2O_2. Finally, the electroactivities of H_2O_2 and O_2 on Pt-black UMEs are intimately related but hard to discriminate upon their reduction waves unless the solution would be analyzed before and after degassing (nitrogen or argon).

3.2 Redox Behavior of Superoxide at pH 12 and its Fate at pH 7.4

The next step consisted in studying the response of Pt-black UMEs towards superoxide anion itself. As described in the experimental section, $O_2^{\bullet-}$ was prepared by solubilizing KO_2 salt in alkaline phosphate buffer (pH 12) in order to stabilize it and therefore facilitate its electrochemical study. Cyclic voltammetry experiments were thus performed in 5 mM superoxide basic solutions (10 mM PBS, pH 12) (Figure 6).

The superoxide anion voltammogram shows a well-defined electrochemical reversible signal on Pt-black surface, which is centered at $E^{\bullet} = -0.085$ V vs Ag/AgCl and follows the redox equation (Equation 4, $O_2/O_2^{\bullet-}$ redox couple):

$$O_2^{\bullet-} \leftrightarrow O_2 + e^- \quad (4)$$

The dependence between the detected electrochemical wave and the superoxide species was further demonstrated by studying the evolution of this response in CV as function of the pH. We first recorded successive CVs in a 5 mM superoxide solution in phosphate buffer at pH 12 for nearly 30 min (40 cycles at 20 mV s^{-1}). A progressive decrease of the wave amplitude was observed (see Figure S3A) even in such basic conditions. $O_2^{\bullet-}$ disproportionates (Equation 1) into dioxygen and hydroperoxide anion (HO_2^-, the basic form of H_2O_2). We performed in parallel a similar experiment in a phosphate buffer solution at pH 12 containing only the hydroperoxide anion and observed that the loss of response was more important for the $O_2^{\bullet-}$ solution (~35 %) than for HO_2^- at pH 12 (~3 %; Figure S3B), as HO_2^- does not follow the disproportionation reaction of $O_2^{\bullet-}$.

This observation was reinforced by switching rapidly the pH of a 5 mM $O_2^{\bullet-}$ solution from 12 to ~7.4, as shown on Figure 6. The evolution was monitored by CV in a potential window where all the different species can be detected, i.e. −0.2 V to +0.5 V. The pH of the superoxide solution was shifted from pH 12 (blue trace) to physiological values (~7.4–7.6) by additions of concentrated HCl (yellow trace). It led to an increase of the reduction current, due to the appearance of O_2 and H_2O_2 formed by the $O_2^{\bullet-}$ decomposition (see Equation 1), while the oxidative current decreased and displayed the oxidation wave of H_2O_2 observed previously (Figure 2). In order to confirm that no more superoxide remained in the solution, SOD (55 U.mL^{-1} final) was added. A very slight increase of reduction and oxidative currents were noticed (purple trace, to be compared with the yellow one), revealing that the major part of superoxide had disproportionated just after the pH change. The shapes of the yellow and purple curves are similar to the one corresponding to an O_2-saturated H_2O_2 solution, as described in Figure 5 (red trace). Thus, at this end stage of the

experiment, H_2O_2 and O_2 should be the only species present in solution.

To verify this later assumption, catalase was added to the solution in order to consume H_2O_2 (orange trace). Compared with the purple trace, the oxidative current due to H_2O_2 oxidation is vanished and the reduction current is decreased leading to a reduction wave attributable to dioxygen (orange trace). Indeed, H_2O_2 was consumed by the catalase producing a stoichiometric amount of O_2 that is reduced at low potentials (see Figures 3 and 5). Overall, this set of experiments unambiguously demonstrates that the reversible wave detected initially at pH 12 is due to superoxide anion.

Moreover, since the electrochemical reaction (equation 4) corresponding to this wave does not involve any proton, superoxide might be detected at the same potentials, with the same Pt-black surfaces, regardless of pH, assuming that the species is sufficiently chemically stable to be detected by CV. When considering the results reported above about the electrochemical responses of superoxide and its relatives, dioxygen and hydrogen peroxide, we may figure out how to discriminate one from the others as a function of the potential window, in particular at pH 7.4. We observed that at potentials below −0.1 V, all three species are reduced on Pt-Black UMEs and cannot actually be discriminated from their CV response. Nevertheless, the addition of scavengers and enzymes (SOD, catalase) would allow to make a decision since the only species remaining after enzymatic conversions is O_2. However, as shown on Figures 2, 5 and 6, at neutral potential, i.e. between 0 and +0.1 V, hydrogen peroxide and oxygen are not detected, only a background current is observed (with slightly negative current values due to the reduction of platinum oxides). Therefore, we can assume that an oxidation current between 0 V and +0.1 V recorded at pH 7.4 would only correspond to superoxide (if produced in sufficient amount). At higher potentials, above +0.1 V, up to +0.5 V herein, $O_2^{\bullet-}$ and H_2O_2 can be both detected meaning that the oxidation current due to H_2O_2 would add to the plateau current of the superoxide oxidation wave already detected at +0.1 V. Consequently, as function of the CV shape and current amplitudes in the range of positive potentials, we might be able to decipher on the contributions of $O_2^{\bullet-}$ and H_2O_2.

This set of analyses opens avenues for the detection of superoxide in aqueous solutions treated by CAPs, for two reasons: 1/ superoxide has already been detected indirectly in plasma-treated solutions [51,52]) and is present transitorily at high concentrations; 2/ CAPs are considered as a source of superoxide (and other RONS) which dissolve at the interface between the gas phase and the liquid solution and does not change significantly the pH of the PBS [19], contrary to the release of superoxide in PBS using the KO_2 source.

In this context, we recently reported [21] the results of *in situ* measurements, with shielded Pt-black UMEs, of species accumulating in PBS exposed to a CAP. We observed in PBS pH 7.4 the progressive appearance of chemically stable species, namely H_2O_2 and NO_2^-, as well as the rise of an oxidation wave and current near 0 V vs Ag/AgCl. This species was detected after long exposure durations (typically 30 min.) of the PBS corresponding to its accumulation and increase of its net flux versus reactions involved in its disappearance. The same experiment was performed in PBS at pH 11, a condition which increases superoxide stability and should favor its steady-state detection. *In situ* monitoring of $O_2^{\bullet-}$ along its generation and accumulation was performed with a shielded Pt-black UME during the solution exposure to a He CAP (see material and methods for details about the setup). As shown in Figure 7, a reversible wave appears after 20 min. and rises in amplitude over the exposure duration. The wave, e.g. detected at 26 min., is very similar in characteristics to the one detected in Figure 6 with the same WE in a solution supplied with the superoxide species. This demonstrates the *in situ* detection of $O_2^{\bullet-}$, which concentration at this time point can be estimated to reach about 400 µM. Moreover, the chemical evolution of superoxide solutions, as discussed above, was also observed in the exposed PBS since a second wave that can very likely be attributed to H_2O_2 was observed after 30 min. The kinetic evolutions of exposed PBS solutions at pH 11 were slower, as expected, than what was observed recently at pH 7.4 [21]. Finally, based on the set of studies reported herein, we draw the conclusion that the species detected in CAP-treated PBS might be superoxide anion. No other RONS (including H_2O_2, $NO^{\bullet}$, $ONOO^-$, HNO and NO_2^-) has shown the same electrochemical and chemical features, particularly when detected with Pt-black modified electrodes.

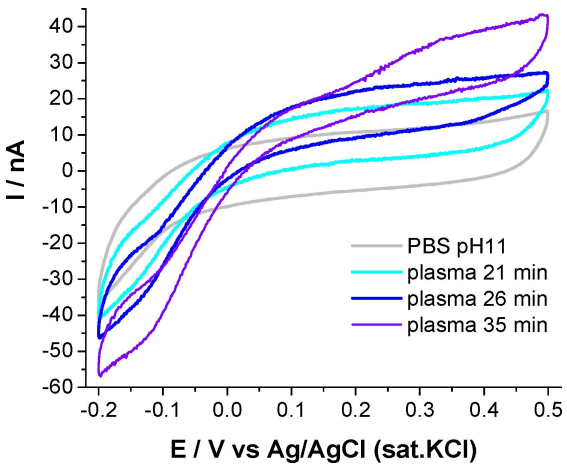

Fig. 7. Evolution of the cyclic voltammetry response in a PBS solution at pH 11 (gray trace, t = 0), along its exposure to a cold atmospheric plasma (He working gas; 100 % N_2 environment). Measurements were performed directly, *in situ* (6 mL cell volume), with a shielded-grounded electrochemical cell (Pt-black UME, REF and CE placed in shielded tubes). Scan rate: 20 mV s^{-1}.

4 Conclusions

In this study, we analyzed the redox behavior of $O_2^{\bullet-}$ in a physiological phosphate-buffered saline (PBS) solution, the most commonly used in bioanalyses. As superoxide is not stable and rapidly disproportionates into H_2O_2 and O_2, it was necessary to decipher on the reactivity of Pt-black UMEs towards these species when they are mixed in solution. We showed that H_2O_2 has a clear redox signature in both oxidation and reduction. Nevertheless, since O_2 is naturally dissolved in solution when working in open environment, the detection by reduction of H_2O_2 appeared to be more complex because its wave overlaps with the one of O_2 reduction. Moreover, we showed that the ORR at Pt-Black (pH 7.4) is a 2 electrons and 2 H^+ process leading to H_2O_2. Thus, oxygen cannot be specifically measured by Pt-black UMEs if hydrogen peroxide is present. However, we have identified that H_2O_2 can be selectively detected with Pt-black UMEs in the potential range of +0.1 V to +0.5 V owing to its first oxidation wave.

The redox response of superoxide on Pt-black UMEs was studied first in alkaline conditions, which favors its stabilization, and then in physiological conditions by changing the pH of the solution. Despite the presence of H_2O_2 and O_2 in solutions at both pH 7.4 and 12, we have identified that 0 V (no overpotential vs Ag/AgCl) is an adequate potential to specifically detect superoxide by Pt-black UMEs based on its oxidation response, regardless of pH. This result opens a range of possibilities concerning the electroanalysis of $O_2^{\bullet-}$ in physiological conditions, for instance when produced by cells in NAPDH oxidase-dependent activities, as well as for biomedical applications of Cold Atmospheric Plasmas (CAPs) produced in air.

Acknowledgements

This work was financially supported by the Centre National de la Recherche Scientifique (CNRS), the French Ministry of Research (MESR) and the Agence Nationale de la Recherche (ANR, PLASMAREGEN project, no. ANR-14-CE16-0007-01).

Data Availability Statement

Data sharing is not applicable to this article as no new data were created or analyzed in this study.

References

[1] H. Sies, D. Jones, *Nat. Rev. Mol. Cell Biol.* **2020**, *21*, 363–383.
[2] I. Liguori, G. Russo, F. Curcio, G. Bulli, L. Aran, D. Della-Morte, G. Gargiulo, G. Testa, F. Cacciatore, D. Bonaduce, P. Abete, *Clin. Interventions Aging* **2018**, *13*, 757–772.
[3] A. Singh, R. Kukreti, L. Saso, S. Kukreti, *Molecules* **2019**, *24*, 1583.
[4] D. Camejo, Á. Guzmán-Cedeño, A. Moreno, *Plant Physiol. Biochem.* **2016**, *103*, 10–23.
[5] J. Navarro-Yepes, M. Burns, A. Anandhan, O. Khalimonchuk, L. M. del Razo, B. Quintanilla-Vega, A. Pappa, M. I. Panayiotidis, R. Franco, *Antioxid. Redox Signaling* **2014**, *21*, 66–85.
[6] G. V. Buxton, C. L. Greenstock, W. P. Helman, A. B. Ross, *J. Phys. Chem. Ref. Data* **1988**, *17*, 513–886.
[7] A. A. Noronha-Dutra, M. M. Epperlein, N. Woolf, *FEBS Lett.* **1993**, *321*, 59–62.
[8] M. Valko, K. Jomova, C. J. Rhodes, K. Kuča, K. Musílek, *Arch. Toxicol.* **2016**, *90*, 1–37.
[9] M. E. Letelier, S. Sánchez-Jofré, L. Peredo-Silva, J. Cortés-Troncoso, P. Aracena-Parks, *Chem.-Biol. Interact.* **2010**, *188*, 220–227.
[10] P. Pacher, J. S. Beckman, L. Liaudet, *Physiol. Rev.* **2007**, *87*, 315–424.
[11] C. Szabó, H. Ischiropoulos, R. Radi, *Nat. Rev. Drug Discovery* **2007**, *6*, 662–680.
[12] A. Privat-Maldonado, A. Schmidt, A. Lin, K.-D. Weltmann, K. Wende, A. Bogaerts, S. Bekeschus, *Oxid. Met.* **2019**, *2019*, 1–29.
[13] S. O. Ganiyu, M. Zhou, C. A. Martínez-Huitle, *Appl. Catal. B* **2018**, *235*, 103–129.
[14] S. Di Meo, T. T. Reed, P. Venditti, V. M. Victor, *Oxid. Met.* **2016**, *2016*, 1–3.
[15] N. K. Kaushik, B. Ghimire, Y. Li, M. Adhikari, M. Veerana, N. Kaushik, N. Jha, B. Adhikari, S.-J. Lee, K. Masur, T. von Woedtke, K.-D. Weltmann, E. H. Choi, *Biol. Chem.* **2018**, *400*, 39–62.
[16] R. Thirumdas, A. Kothakota, U. Annapure, K. Siliveru, R. Blundell, R. Gatt, V. P. Valdramidis, *Trends Food Sci. Technol.* **2018**, *77*, 21–31.
[17] K.-D. Weltmann, T. von Woedtke, *Plasma Phys. Controlled Fusion* **2017**, *59*, 014031.
[18] X. Chen, F. Wang, J. Y. Hyun, T. Wei, J. Qiang, X. Ren, I. Shin, J. Yoon, *Chem. Soc. Rev.* **2016**, *45*, 2976–3016.
[19] F. Girard, V. Badets, S. Blanc, K. Gazeli, L. Marlin, L. Authier, P. Svarnas, N. Sojic, F. Clément, S. Arbault, *RSC Adv.* **2016**, *6*, 78457–78467.
[20] F. Girard, M. Peret, N. Dumont, V. Badets, S. Blanc, K. Gazeli, C. Noël, T. Belmonte, L. Marlin, J.-P. Cambus, G. Simon, N. Sojic, B. Held, S. Arbault, F. Clément, *Phys. Chem. Chem. Phys.* **2018**, *20*, 9198–9210.
[21] F. Girard-Sahun, V. Badets, P. Lefrançois, N. Sojic, F. Clement, S. Arbault, *Anal. Chem.* **2019**, *91*, 8002–8007.
[22] C. Calas-Blanchard, G. Catanante, T. Noguer, *Electroanalysis* **2014**, *26*, 1277–1286.
[23] E. Suraniti, S. Ben-Amor, P. Landry, M. Rigoulet, E. Fontaine, S. Bottari, A. Devin, N. Sojic, N. Mano, S. Arbault, *Angew. Chem.* **2014**, *126*, 6773–6776; *Angew. Chem. Int. Ed.* **2014**, *53*, 6655–6658.
[24] P. Manning, C. J. McNeil, *Biochem. Soc. Trans.* **2011**, *39*, 1288–1292.
[25] F. Bedioui, D. Quinton, S. Griveau, T. Nyokong, *Phys. Chem. Chem. Phys.* **2010**, *12*, 9976.
[26] S. Gáspár, J. L. Marty, E. Gheorghiu, *Electroanalysis* **2013**, *25*, 448–452.
[27] C. Amatore, S. Arbault, A. C. W. Koh, *Anal. Chem.* **2010**, *82*, 1411–1419.
[28] C. Amatore, S. Arbault, C. Bouton, J.-C. Drapier, H. Ghandour, A. C. W. Koh, *ChemBioChem* **2008**, *9*, 1472–1480.
[29] C. Amatore, S. Arbault, Y. Bouret, B. Cauli, M. Guille, A. Rancillac, J. Rossier, *ChemPhysChem* **2006**, *7*, 181–187.

[30] C. Amatore, S. Arbault, D. Bruce, P. De Oliveira, M. Erard, M. Vuillaume, *Chem. Eur. J.* **2001**, *7*, 4171–4179.
[31] R. Hu, M. Guille, S. Arbault, C. J. Lin, C. Amatore, *Phys. Chem. Chem. Phys.* **2010**, *12*, 10048–10054.
[32] L. Xiang, P. Yu, M. Zhang, J. Hao, Y. Wang, L. Zhu, L. Dai, L. Mao, *Anal. Chem.* **2014**, *86*, 5017–5023.
[33] Y. Li, A. Meunier, R. Fulcrand, C. Sella, C. Amatore, L. Thouin, F. Lemaître, M. Guille-Collignon, *Electroanalysis* **2016**, *28*, 1865–1872.
[34] Y. Li, C. Sella, F. Lemaître, M. Guille Collignon, L. Thouin, C. Amatore, *Electroanalysis* **2013**, *25*, 895–902.
[35] Y. Li, C. Sella, L. Thouin, *Anal. Chem.* **2018**, 9.
[36] Y. Li, C. Sella, F. Lemaître, M. Guille-Collignon, L. Thouin, C. Amatore, *Electrochim. Acta* **2014**, *144*, 111–118.
[37] V. Badets, J. Pandard, N. Sojic, S. Arbault, *ChemElectroChem* **2016**, *3*, 2288–2296.
[38] S. Marklund, *J. Biol. Chem.* **1976**, *251*, 7504–7507.
[39] S. Ben-Amor, E. Vanhove, F. Sékli Belaïdi, S. Charlot, D. Colin, M. Rigoulet, A. Devin, N. Sojic, J. Launay, P. Temple-Boyer, S. Arbault, *Electrochim. Acta* **2014**, *126*, 171–178.
[40] K. T. Kawagoe, J. A. Jankowski, R. Mark. Wightman, *Anal. Chem.* **1991**, *63*, 1589–1594.
[41] I. Katsounaros, W. B. Schneider, J. C. Meier, U. Benedikt, P. U. Biedermann, A. A. Auer, K. J. J. Mayrhofer, *Phys. Chem. Chem. Phys.* **2012**, *14*, 7384.
[42] X. Cai, E. E. L. Tanner, C. Lin, K. Ngamchuea, J. S. Foord, R. G. Compton, *Phys. Chem. Chem. Phys.* **2018**, *20*, 1608–1614.
[43] I. Katsounaros, W. B. Schneider, J. C. Meier, U. Benedikt, P. U. Biedermann, A. A. Auer, K. J. J. Mayrhofer, *Phys. Chem. Chem. Phys.* **2012**, *14*, 7384–7391.
[44] C. H. Choi, H. C. Kwon, S. Yook, H. Shin, H. Kim, M. Choi, *J. Phys. Chem. C* **2014**, *118*, 30063–30070.
[45] Y. Jiang, P. Ni, C. Chen, Y. Lu, P. Yang, B. Kong, A. Fisher, X. Wang, *Adv. Energy Mater.* **2018**, *8*, 1801909.
[46] Md. T. Islam, Md. M. Hasan, Md. F. Shabik, F. Islam, Y. Nagao, M. A. Hasnat, *Electrochim. Acta* **2020**, *360*, 136966.
[47] Md. S. Hossain, M. Y. A. Mollah, Md. A. B. H. Susan, Md. M. Islam, *Electrochim. Acta* **2020**, *344*, 136146.
[48] M. A. Hasnat, A. J. Gross, S. E. C. Dale, E. O. Barnes, R. G. Compton, F. Marken, *The Analyst* **2014**, *139*, 569–575.
[49] V. Badets, J. Pandard, N. Sojic, S. Arbault, *ChemElectroChem* **2016**, *3*, 2288–2296.
[50] C. Amatore, S. Arbault, C. Ducrocq, S. Hu, I. Tapsoba, *ChemMedChem* **2007**, *2*, 898–903.
[51] J. Chauvin, F. Judée, M. Yousfi, P. Vicendo, N. Merbahi, *Sci. Rep.* **2017**, *7*, DOI 10.1038/s41598-017-04650–4.
[52] A. Khlyustova, C. Labay, Z. Machala, M.-P. Ginebra, C. Canal, *Front. Chem.* **2019**, *13*, 238–252.

Received: October 15, 2020
Accepted: November 5, 2020
Published online on ■■, ■■

FULL PAPER

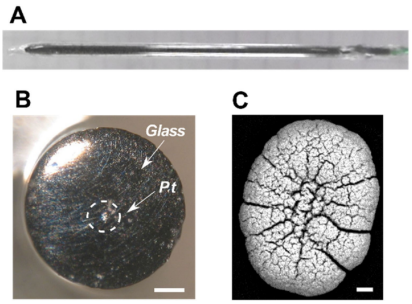

*P. Lefrançois, F. Girard-Sahun, V. Badets, F. Clément, S. Arbault**